International Journal of Thermophysics, Vol. 20, No. 3, 1999

Critical Behavior of O_2^- Ions in Argon Gas[1]

A. F. Borghesani,[2,3] D. Neri,[2] and A. Barbarotto[2]

We measured the drift mobility of O_2^- ions in argon gas close to the critical point for $(1.005 < T/T_c < 1.04)$ above $T_c \approx 150.7$ K in the density range $(0.025 < N/N_c < 1.733)$ around the bulk critical density $N_c = 8.08$ atoms $\cdot$ nm^{-3}. The density-normalized zero-field mobility $\mu_0 N$ of the ions shows a deep minimum as a function of the gas density N as $T \to T_c^+$. This anomalous reduction of $\mu_0 N$ occurs at a density $N_m \approx 0.76 N_c$. We believe that this behavior is due to the strong electrostriction exerted by the ion on the highly compressible gas. By introducing suitable contributions to the effective ion radius R due to the large gas compressibility and taking into account short-range local density and viscosity augmentation due to electrostriction, the hydrodynamic Stokes formula $\mu_0 = e/6\pi\eta R$, where η is the gas viscosity, is in good agreement with the experimental data.

KEY WORDS: electrostriction; hydrodynamic drag; ion drift mobility; kinetic theory.

1. INTRODUCTION

The motion of ions in fluids is studied to investigate the ion–atom interaction in different environments. In low-density gases the ion–atom potential is determined from drift mobility data using kinetic theory [1]. In liquids, the mobility depends on the microscopic fluid structure and is described by hydrodynamics [2]. Less attention has been devoted to dense gases, even though the density can be varied in a large interval, permitting an investigation of the limits of applicability of either description of the ionic motion. Moreover, there is a lack of investigations at the liquid–vapor

[1] Paper presented at the Thirteenth Symposium on Thermophysical Properties, June 22–27, 1997, Boulder, Colorado, U.S.A.

[2] Istituto Nazionale per la Fisica della Materia, Dipartimento di Fisica "G. Galilei," University of Padua, Via F. Marzolo 8, I-35131 Padua, Italy

[3] To whom correspondence should be addressed.

0195-928X/99/0500-0899$16.00/0

critical point [3, 4], where the transport coefficients show an anomalous behavior [5].

Positive ions are more carefully studied because they are easily produced by ionization. Their structure and transport properties are known. Electrostriction exerted on the polarizable medium by the electric field of the ion enhances the local density around it. The attraction strength increases with increasing gas atomic polarizability, α, and with decreasing temperature T, and may cause the fluid to locally solidify [6] or the ion to be surrounded by a solvation cluster. So the ion transport depends on the hydrodynamic interaction with the fluid of the large structure surrounding the ion.

Impurity negative ions are not equally well known. Among them, O_2^- is very important because O_2 is a very common electron-scavenging impurity. Its mobility μ in dense gases has been studied as a function of the bulk gas density N in ^{4}He at $T=77$ K [7, 8]. The neighborhood of the critical point has been investigated in neon [4] at $T\approx 45$ K ($T/T_c\approx 1.04$) in an extended density range ($0.1\leqslant N/N_c\leqslant 1.7$). Important features of the zero-field density-normalized mobility $\mu_0 N$ in neon are a weak minimum at a reduced density $N/N_c\approx 0.72$ and the absence of any anomaly for $N=N_c$. A similar behavior is shown by $^3He^+$ in ^{3}He at $T/T_c\geqslant 1.001$ [9], where, for $N\approx 0.9N_c$, $\mu_0 N$ has a stronger minimum. The smaller effect in neon is due to the competition between the larger ion–atom attractive interaction ($\alpha_{Ne}\approx 2\alpha_{He}$) and the higher thermal energies ($T_{Ne}\approx 15T_{^3He}$). Moreover, the behavior of $\mu_0 N$ in neon is quite complicated. For low to medium N ($0.15\leqslant N/N_c\leqslant 0.43$), $\mu_0 N$ is nearly independent of N. Then it decreases towards the minimum for $N/N_c\approx 0.72$. Finally, $\mu_0 N$ increases until $N/N_c\approx 1.4$, where it saturates to a value twice as large as its low-density value [4]. The dependence of $\mu_0 N$ on N was not satisfactorily explained [4, 7]. For the high-N region, it was assumed [4] that μ_0 is described by the Stokes formula,

$$\mu_0=\frac{e}{6\pi\eta R} \tag{1}$$

where η is the bulk gas viscosity and R is the ion radius. Electrostriction is taken into account by solving the Navier–Stokes equation in presence of the nonuniformities surrounding the ion, yielding $\mu_0=e/6\pi\eta RF$ [10]. The factor $F\approx 1$ depends on the temperature T, on N, and on the shape of the local density and viscosity profiles, but the agreement with experiment is poor.

On the basis of Eq. (1), μ_0 is expected to mirror the critical divergence of η [11], which is, however, very weak and cannot account for a mobility

minimum located at an off-critical density. Therefore, the experiments seem to confirm the theory of Watanabe [12], where heavy ions, interacting with atoms through a contact potential, are not elastically scattered off long-wavelength density fluctuations. Ions are not coupled to them because the relevant length scales, the correlation length ξ of fluctuations and the ion thermal wavelength ($\lambda_T \approx 0.02$ nm) are too different. Moreover, the ion thermal velocity is such that the time spent by an ion passing through a fluctuation is much less than the decay time of fluctuations so that their dissipative properties do not influence μ_0.

A model has been proposed [13], where the quantum nature of the interaction between the gas atoms and the additional electron in the O_2^- ion is considered to describe the ion mobility. This electron is weakly bound, and its orbit is extended in space. The competition between short-range repulsive exchange forces and the long-range polarization interaction forms an empty cavity around the ion, surrounded by a region of enhanced gas density. The strength and shape of this density augmentation are related to α and to the gas compressibility, χ_T, and are relevant close to the critical point [6, 13, 14]. μ_0 is well described in helium [7], where α is so small that only an empty void surrounds the ion, but not in neon [4], where α is larger and the density enhancement is strong. The neon data are reproduced almost quantitatively for $N \geqslant N_c$ by assuming the validity of Eq. (1), by taking the position of the maximum of the density profile as the hydrodynamic radius R, and by using the local viscosity value corresponding to the density maximum. However, the data for $N < N_c$ are not reproduced.

We have therefore investigated argon because, due to its large α, a strong density enhancement around the ion is expected. Argon should represent a valid test of Watanabe's theory. We show that the $\mu_0 N$ of O_2^- is strongly affected by the critical point of argon, probably through the formation of a layer of correlated fluid around the ion. Preliminary results have been published [15].

2. EXPERIMENT

We used the pulsed electron photoinjection technique exploited for mobility measurements of O_2^- ions in helium and neon [4, 8]. The cell containing the gas is thermoregulated within ± 0.01 K. Thermal gradients are estimated to be $< 2\ \mathrm{K \cdot m^{-1}}$. T is measured with a calibrated Pt resistor. The absolute value of T is known within ± 0.3 K. The gas pressure P is measured with an uncertainty of ± 1 kPa. N is calculated from P and T using a recent equation of state [16]. Two parallel-plate electrodes,

separated by a distance $d = 10$ mm, are irradiated with a short UV light pulse. The extracted photoelectrons are captured by O_2 impurities, at a concentration of some tens of ppm, to form O_2^- ions. The ionic drift time τ_i is obtained by analyzing the signal waveform produced by the ion motion. μ is given by $\mu = d^2/\tau_i V$, where V is the applied voltage. The uncertainty on μ is $\approx 5\%$.

3. RESULTS AND DISCUSSION

For electric fields $E \leqslant 0.3$ MV $\cdot$ m^{-1}, μ is nearly field independent, equal to its zero-field value, μ_0 (Fig. 1). This is because ions are near thermal equilibrium with the gas atoms. However, the change in the density dependence of $\mu_0 N$, as $T \to T_c^+$, is striking. For $T = 180$ K $\gg T_c = 150.7$ K, $\mu_0 N$ increases linearly with N (Fig. 2). This behavior is also shown at higher T and is also observed in neon [7, 8] and helium [4, 8]. For $T = 157$ K ($T/T_c \approx 1.04$), the slope changes sign and $\mu_0 N$ decreases linearly with increasing N. Moreover, a small depression in the region $0.5 \leqslant N/N_c \leqslant 1.1$ is superimposed on the linear decrease in $\mu_0 N$ (Fig. 2). For $T = 154$ K ($T/T_c \approx 1.02$), the small depression of $\mu_0 N$ has developed into a well-defined, though broad, minimum centered about $N/N_c \approx 0.76$. Finally, for $T = 151.5$ K ($T/T_c \approx 1.005$), the $\mu_0 N$ minimum located at $N_m = 0.76 N_c$ has become very deep (Fig. 3).

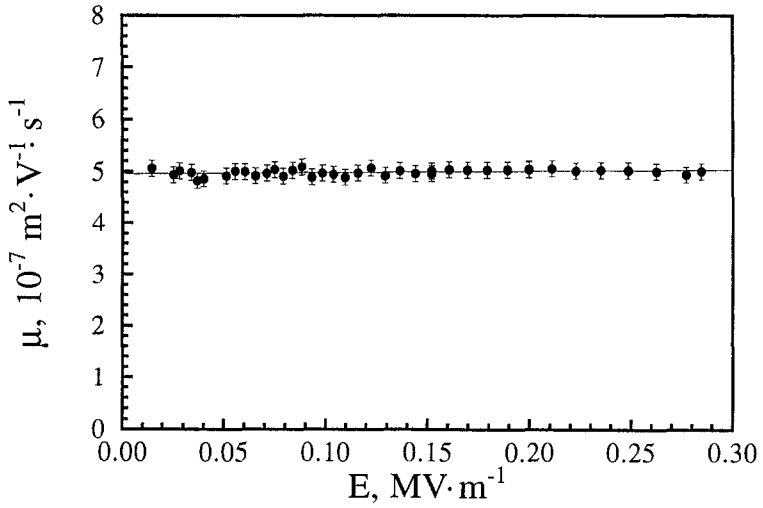

Fig. 1. Electric field dependence of the O_2^- ion mobility μ for $N = 5.83$ atoms $\cdot$ nm^{-3} ($N/N_c = 0.722$) at $T = 154$ K.

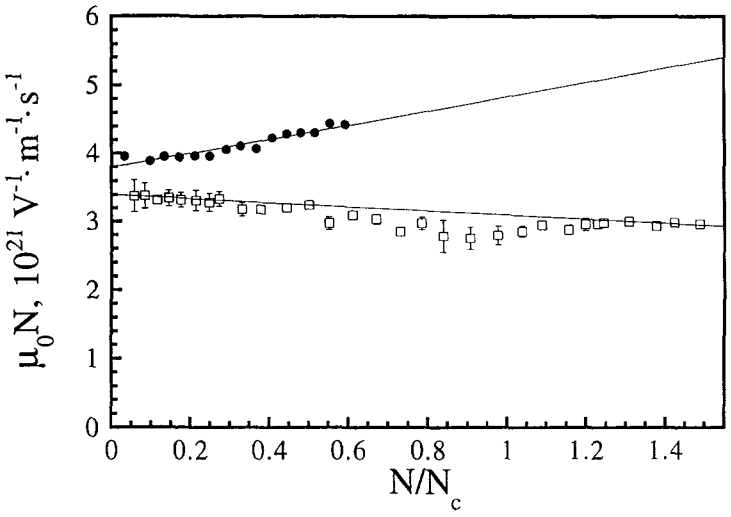

Fig. 2. Density-normalized zero-field mobility $\mu_0 N$ as a function of the reduced density N/N_c. Filled circles, $T = 180$ K; open squares: $T = 157$ K. The solid lines are only a guide for the eye.

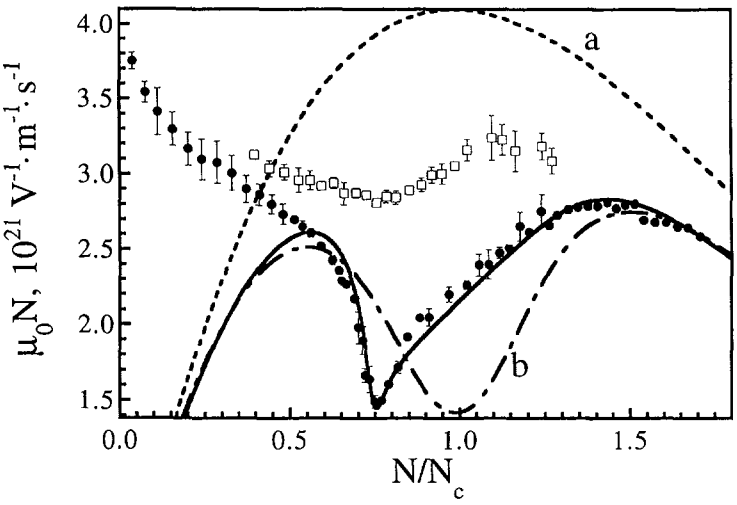

Fig. 3. $\mu_0 N$ as a function of N/N_c for $T = 154$ K (open squares) and for $T = 151.5$ K (filled circles). Curve a is the prediction of Eq. (1). Curve b is the prediction of Eq. (1) with R given by Eq. (2). The solid curve is the prediction of Eq. (1) with R given by Eq. (4).

Interestingly, the minimum develops and deepens as $T \to T_c^+$, although it is located at a definitely off-critical N. This behavior bears similarities with the results of other experimental [17–21], as well as theoretical [22] and simulation [23–25], studies concerning the solvation of a molecular solute in supercritical fluids (SCF). The electrostatic interaction between solute and solvent in a highly compressible SCF dramatically alters the solute environment. A number of solvent atoms clusters around the solute, largely enhancing the local solvent density. Solvatochromic studies have been widely carried out because they are inherently sensitive to local, structural solvent effects. The modification of the local solute environment due to clustering also influences the solute dynamics. For example, the correlation time of the rotational relaxation of a solute, described by a modified Stokes–Debye–Einstein equation, provides a measure of the microscopic solvent–solute friction, and in the compressible region of a SCF, it is expressed in terms of an enhanced local density [26–28].

The failure of the Stokes–Einstein hydrodynamic equation, relating the diffusion coefficient D of the solute to the solvent viscosity η, at low N in a SCF might be due to the formation of a cluster around the solute that modifies its hydrodynamic size. The same kind of failure affected also the results of experiments which, exploiting the relationship between the diffusion coefficient, D, and drag coefficient of a sphere of radius R, $D = k_B T/6\pi\eta R$, valid even for microscopic brownian particles [29], were aimed at the determination of the η anomaly in binary mixtures at the consolute critical point. Different results were obtained, depending on the degree of the particle–liquid interaction. Agreement with the viscometric determinations of η were obtained by assuming that a layer of correlated fluid surrounds the particles, enhancing their hydrodynamic radius, and that its thickness is proportional to the correlation length ξ of critical fluctuations [30].

Here, assuming the validity of Eq. (1), we obtain the ion effective hydrodynamic radius R from $\mu_0 N$. The dependence of η on N is found in the literature [31]. In Fig. 4 we show R as a function of N/N_c for $T = 151.5$ K. R is maximum for N_m, where $\mu_0 N$ is minimum. For $N/N_c \approx 0.37$, $R \approx 0.5$ nm, close to the value $R_1 \approx 0.46$ nm of one solvation shell of argon atoms (the Ar–Ar interaction hard-core radius is $\sigma_A = 0.34$ nm and that of the $O_2^- - At$ interaction can be estimated to be $\sigma_o \approx 0.29$ nm [32,33]). For $N/N_c \approx 1.73$, $R \approx 0.76$ nm, close to the value $R_2 \approx 0.82$ nm of two solvation shells.

Because of the electrostriction effect induced by the ionic charge on the polarizable atoms of the highly compressible fluid, a number of excess solvent atoms gather around the ion, and their motion is locally correlated

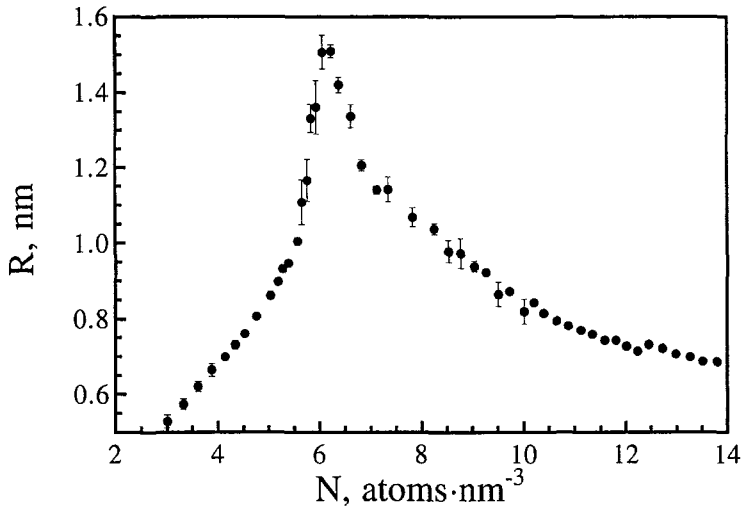

Fig. 4. Hydrodynamic ion radius R calculated from μ_0 by means of Eq. (1) for $T = 151.5$ K as a function of N/N_c.

with that of the ion, thus altering its hydrodynamic drag. Therefore, the ion effective hydrodynamic radius provides a measure of its degree of solvation. In this sense there is a close relationship between the behavior of μ_0 in this experiment and the local density augmentation phenomena investigated in solvatochromic studies. These phenomena are interpreted in terms of the formation of long-lived clusters of solvent around the solute, i.e., the formation of a local enhancement of the solvent density around the solute induced by the solute–solvent interaction. The main feature of this phenomenon [17, 34] is that its maximum appears at a density below the bulk critical density of the pure fluid and does not coincide with the maximum in χ_T. Therefore, these effects are argued to be due to solvation rather than to criticality.

Unfortunately, one poorly investigated issue is how the local density augmentation is affected by the approach to T_c. There is experimental evidence that it is enhanced as $T \to T_c^+$ [17], although this observation remains largely unexplained. The same effect is observed here, where the approach to T_c enhances the mobility drop. Our experiment, therefore, puts into evidence that, near the bulk critical temperature of the solvent, the solvation effects, although short-ranged, are strongly affected by the long-range, critical phenomenon. This point of view is supported by the strong mobility change observed between the investigated isotherms as $T \to T_c^+$ smoothly.

No model has been devised yet to explain the ion mobility by taking into account this evidence. To describe the behavior of $\mu_0 N$, we assume that a fluid layer of thickness $\propto \xi$ is dragged by the ion. In the critical region $\xi \propto S^{1/2}(0)$, where $S(0) = Nk_B T\chi_T$ is the long-wavelength limit of the static structure factor. Therefore, we heuristically put

$$R = a_0 + a_1 N + a_2 S^{1/2}(0) \tag{2}$$

where a_0, a_1, and a_2 are fitting parameters. The linear contribution $(a_0 + a_1 N)$ interpolates linearly between the radii of one and two solvation shells. The contribution $\propto S^{1/2}(0)$ is relevant close to the critical point. By using Eq. (2), we obtain curve b in Fig. 3. This curve shows a minimum for $N = N_c$, where $S(0)$ is maximum, in contrast to the experiment. The reason for the discrepancy is that $S(0)$ is a thermodynamic property of the unperturbed gas and is therefore a long-range property uncorrectly used to describe a local property of the fluid structure around the solute. Electrostriction modifies the fluid properties around the solute by enhancing the local density N_r and viscosity $\eta_r \equiv \eta(N_r)$ at a distance r from the ion, and the hydrodynamic drag depends on the local values of the fluid properties. A similar approach is used to interpret the rotational dynamics of molecular solutes in SCF [26–28].

The local density and viscosity profiles around the ion induced by electrostriction can be explicitly calculated by using continuum models [6, 14], which are, however, highly questionable, in particular, near the solvent critical point, because short- and long-range effects are mixed. Moreover, these models assume that the local fluid properties, though varying on a scale comparable to ξ, can still be calculated from bulk thermodynamics. Nonetheless, we first recall that in this experiment no measurements were carried out along the critical isochore. Therefore, we do not expect that the conditions for ξ to diverge are truly met. Second, we observe that the ion–atom r^{-4} potential has a longer range than the r^{-6} tail of the argon–argon interaction that determines the scale against which ξ has to be compared. Finally, in the absence of any reliable theory we would like to put forward a heuristic model in order to suggest a possible physical interpretation of our observations. Its validity will be ascertained a posteriori by the degree of agreement with the experiment. We thus assume that the local density profile is given by [6],

$$-V(r) = K^2(N_r) \int_N^{N_r} \left(\frac{\partial P}{\partial N}\right)_T d \ln N \tag{3}$$

where $V(r)$ is the ion–atom potential and $K(N_r)$ is the local dielectric constant of the gas. N_r is the density value at a distance r from the ion. A typical

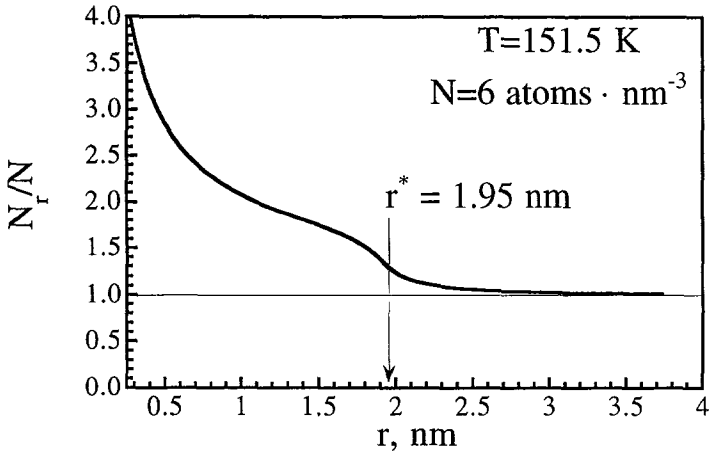

Fig. 5. Electrostriction induced local argon density profile around the ion for $N = 6$ atoms $\cdot$ nm^{-3} ($N/N_c = 0.75$) and $T = 151.5$ K. A 12-6-4 argon–ion interaction potential with a hard-core radius $\sigma = 0.29$ nm and a well depth of 1.57×10^{-20} J was used.

density profile is shown in Fig. 5. If $N < N_c$, $N_r = N_c$ at a given distance from the ion, where the local value S_r of $S(0)$ is maximum, though finite. Assuming that the hydrodynamic radius is

$$R = a_0 + a_1 N + a_2 S_r^{1/2} \tag{4}$$

instead of Eq. (2), the maximum of R occurs for $N = N_m$, if the local properties are evaluated for $r = r^* = 1.95$ nm for any N. Accordingly, in Eq. (1), the local value of η, η_r at $r = r^*$, is used. The best agreement with the data (solid line in Fig. 3) is obtained for $a_0 = 0.56$ nm, $a_1 = 4.4 \times 10^{-3}$ nm^4 $\cdot$ atoms^{-1}, and $a_2 = 0.55$ nm. The agreement of this modified Stokes formula with the data is good, even for quite low N ($N/N_c \approx 0.5$). In Fig. 3 we also show the results of Eq. (1) (curve a) obtained by using the bulk viscosity and the linear term $R = 0.56 + 4.4 \times 10^{-3} N$, only. The disagremeent with the data clearly shows the relevance of the contribution of the correlated fluid layer and the importance of using local values for the fluid properties.

The agreement of this model with the data supports the conclusion that the effective hydrodynamic radius of the ion, though related to short-range solvation effects, is strongly affected by the approach to T_c, probably because of the coupling of the ion–atom polarization interaction with density fluctuations and also indicates that a contact potential is a bad approximation.

Finally, we point out that the hydrodynamic description of the ionic mobility fails for $N/N_c \leqslant 0.5$, where a different transport mechanism is clearly active. A more detailed theoretical analysis of the momentum transfer mechanisms in the transition regime from kinetic to hydrodynamic is still needed to describe fully the density dependence of the ion mobility.

REFERENCES

1. E. A. Mason and E. W. McDaniel, *Transport Properties of Ions in Gases* (Wiley, New York, 1988).
2. H. T. Davis, S. A. Rice, and L. Meyer, *J. Chem. Phys.* **37**:947 (1962).
3. N. Gee, S. S.-S. Huang, T. Wada, and G. R. Freeman, *J. Chem. Phys.* **77**:1411 (1982).
4. A. F. Borghesani, D. Neri, and M. Santini, *Phys. Rev.* **E48**:1379 (1993).
5. K. Kawasaki and J. D. Gunton, *Critical Dynamics* in *Progress in Liquid Physics*, C. A. Croxton, ed. (Wiley, New York, 1978), p. 175.
6. K. R. Atkins, *Phys. Rev.* **116**:1339 (1959).
7. A. K. Bartels, *Appl. Phys.* **8**:59 (1975).
8. A. F. Borghesani, F. Chiminello, D. Neri, and M. Santini, *Int. J. Thermophys.* **16**:1235 (1995).
9. R. M. Ostermeier and K. W. Schwarz, *Phys. Rev. A* **5**:2510 (1972).
10. R. Cantelli, I. Modena, and F. P. Ricci, *Phys. Rev.* **171**:236 (1968).
11. R. F. Berg and M. R. Moldover, *J. Chem. Phys.* **93**:1926 (1990).
12. S. Watanabe, *J. Phys. Soc. (Japan)* **46**:1819 (1979).
13. K. F. Volykhin, A. G. Khrapak, and W. F. Schmidt, *JETP* **81**:901 (1995).
14. J. R. Quint and R. H. Wood, *J. Phys. Chem.* **89**:380 (1985); R. H. Wood, J. R. Quint, and J.-P. Grolier, *J. Phys. Chem.* **85**:3944 (1981).
15. A. F. Borghesani, D. Neri, and A. Barbarotto, *Chem. Phys. Lett.* **267**:116 (1997).
16. C. Tegeler, R. Span, and W. Wagner, *VDI Fortschritt-Berichte*, Reihe 3, Nr. 480 (VDI Verlag, Düsseldorf, 1997).
17. J. Zhang, L. L. Lee, and J. F. Brennecke, *J. Phys. Chem.* **99**:9268 (1995).
18. C. Carlier and T. W. Randolph, *AIChE J.* **39**:876 (1993).
19. J. Zhang, D. P. Roeck, J. E. Chateauneuf, and J. F. Brennecke, *J. Am. Chem. Soc.* **119**:9980 (1997).
20. Y. P. Sun, G. Bennett, K. P. Johnston, and M. A. Fox, *J. Phys. Chem.* **96**:10001 (1992).
21. J. Bryan Ellington, K. M. Park, and J. F. Brennecke, *Ind. Eng. Chem. Res.* **33**:965 (1994).
22. K. P. Johnston, G. E. Bennett, P. B. Balbuena, and P. J. Rossky, *J. Am. Chem. Soc.* **118**:6746 (1996).
23. I. B. Petsche and P. G. Debenedetti, *J. Chem. Phys.* **91**:7075 (1989).
24. J. A. O'Brien, T. W. Randolph, C. Carlier, and S. Ganapathy, *AIChE J.* **39**:1061 (1993).
25. L. W. Flanagin, P. B. Balbuena, K. P. Johnston, and P. J. Rossky, *J. Phys. Chem. B* **101**:7998 (1997).
26. R. M. Anderton and J. F. Kauffmann, *J. Phys. Chem.* **98**:12117 (1994).
27. R. M. Anderton and J. F. Kauffmann, *J. Phys. Chem.* **99**:13759 (1995).
28. M. P. Heitz and F. V. Bright, *J. Phys. Chem.* **100**:6889 (1996).
29. G. L. Pollack, *Phys. Rev. A* **23**:2660 (1981).
30. K. B. Lyons, R. C. Mockler, and W. J. O'Sullivan, *Phys. Rev. Lett.* **30**:42 (1973).

31. N. J. Trappeniers, P. S. van der Gulik, and H. van den Hooff, *Chem. Phys. Lett.* **70**:438 (1980).
32. G. C. Maitland, M. Rigby, E. B. Smith, and W. A. Wakeham, *Intermolecular Forces. Their Origin and Determination* (Clarendon Press, Oxford, 1981).
33. A. Barbarotto, Tesi di Laurea (University of Padua, 1996), unpublished.
34. A. O'Brien, T. W. Randolph, C. Carlier, and S. Ganapathy, *AIChE J.* **39**:1061 (1993).